Electrochemical oxidation as alternative for dissolution of metal oxides in deep eutectic solvents

Ioanna M. Pateli,[a,b] Andrew P. Abbott,[a] Gawen R. T. Jenkin,[c] Jennifer M. Hartley [a]*

[a] School of Chemistry, University of Leicester, Leicester, LE1 7RH, UK

[b] Stephenson Institute for Renewable Energy, University of Liverpool, Liverpool, L69 7ZF, UK

[c] School of Geography, Geology and the Environment, University of Leicester, Leicester, LE1 7RH, UK

* Contact email: jmh84@le.ac.uk

Abstract

Metal oxide dissolution is central to most metal processing and is generally carried out using mineral acids. An alternative approach has been demonstrated for metal sulfides using electrochemical oxidation. Here the so-called paint casting method was employed to investigate the electrochemical dissolution and recovery of selected metal oxides. Cyclic voltammetry showed that all of the metal oxides were electrochemically active in deep eutectic solvent media, and the majority displayed a redox couple that could be potentially assigned to the redox behaviour of the oxide moiety. Bulk anodic dissolution was carried out on the metal oxides, and it was shown that dissolution was enhanced to up to >10,000 times in pH neutral solutions. The rate of electrochemical dissolution was shown to be influenced by the band gap of the compounds. It is proposed that oxidation of the oxide moiety, potentially to the superoxide, enables the solubilisation of the metal ions. The metal speciation appears to remain the same as for chemical dissolution.

Keywords

Superoxide; cyclic voltammetry; metal oxides; deep eutectic solvents

Introduction

Metal oxides (MOs) are ubiquitous in minerals and consumer products and their processing for metal extraction and waste processing is one of the largest industrial sectors. Pyrometallurgical methods are commonly used to recover metals from high metal content ores using temperatures >1200°C. Pyrometallurgy is also used for recycling of MOs from end-of-life products such as lithium ion batteries.[1] Lower grade ores and more complex minerals are more commonly processed via hydrometallurgy, requiring the use of large volumes of acidic or basic solutions, frequently with the addition of complexing, oxidising or reducing agents. Both of these methods have significant environmental footprints and they face different issues such as the release of greenhouse gases, high energy consumption and production of often hazardous aqueous and solid wastes, requiring treatment prior to disposal.[2] Hence, alternative technologies for MO extraction, such as ionometallurgy and solvometallurgy have been investigated.[3, 4]

Ionometallurgy describes a group of methods using ionic media, such as molten salts, ionic liquids (ILs) and deep eutectic solvents (DESs) for the extraction and recovery of metals.[5] DESs are eutectic mixtures of quaternary ammonium salts and hydrogen bond donors (HBDs)[6] and are solvents of interest for metal extraction, due to their high thermal and chemical stability, lower toxicity, non-flammability, non-volatility and wide liquid window compared to aqueous solutions. In addition, their higher electrochemical stability compared to aqueous solutions is an advantage for electrochemical metal recovery.[7] Metal leaching from MOs has been investigated in ILs,[8-15] as well as DESs,[3, 16-29] either in fundamental studies, or from industrial residues such as lithium ion batteries and fluorescent lamp wastes. While the properties of both DESs and ILs can be 'tuned' by judicious selection of cation, anion, and HBD, resulting in more selective processes compared to hydrometallurgy, the use of DESs is preferable due to their lower cost of production, lower toxicity and higher biodegradability. From previous research,[29] it was concluded that the leaching of MOs in DESs is highly influenced by both the proton activity of the solvent and the coordination properties of any potential ligands in solution. However, leaching can be slow due to a combination of chemical (e.g. low concentrations of H^+ or suitable ligands) or physical (e.g. solvent viscosity) factors. Slow chemical leaching can be bypassed by electrochemical dissolution, either oxidative or reductive, as shown for aqueous systems through the use of Pourbaix diagrams.[30] The efficiency of this approach depends on the possible oxidation states of the metal and the conductivity of the MO.[31]

Electrochemical processing of MOs in ionic media has often focused on reducing the metal cation of the MO, and has been widely studied in molten salts due to their stability over a wide applied voltage range, especially for reactive metals such as Ti in the Fray-Farthing-Chen (FFC) Cambridge process.[32-34] In lower temperature DES systems, the electrochemical reduction of copper[35] and lead[36] oxides to the metal has also been demonstrated. The issue with this approach is that all of the oxide needs to be reduced or it can become incorporated into the metal product.

The oxidation of MOs in ionic media is less well-studied than the reduction of MOs, however experiments into the oxidation of other metal chalcogenides, such as metal sulfides,[37, 38] selenides and tellurides,[39] have been carried out. It was observed that the chalcogenide could be oxidised to the highest oxidation states possible, i.e. forming SO_4^{2-}, SeO_4^{2-} and TeO_4^{2-}.[39] Based on these observations, it would be interesting to investigate if oxide is also electrochemically active in DES media. In this investigation, the electrochemical oxidative dissolution of MnO_2, MnO, Fe_2O_3, Fe_3O_4, Co_3O_4, CoO, NiO, CuO, Cu_2O, ZnO and PbO in DESs is studied by electrochemical oxidative dissolution in EG:ChCl, using a paint casting method.[40] The aim is to investigate whether metallic elements can be recovered from oxides through electro-oxidation accompanied by subsequent electro-reduction of the liberated metal ions.

Experimental

Chemicals and DES preparation

The MOs used in this investigation were: MnO_2 (Acros Organics, 99%), MnO (Alfa Aesar, 78%), Fe_2O_3 (Alfa Aesar, 96%), Fe_3O_4 (Aldrich, 97%), Co_3O_4 (Alfa Aesar, 99%), CoO (Alfa Aesar, 95%), NiO (Alfa Aesar, 99%), CuO (Chem Cruz, 99%), Cu_2O (Alfa Aesar, 99%), ZnO (AnalaR, 99.5%) and PbO (Alfa Aesar, 99.9%). The components of the deep eutectic solvent were: choline chloride (ChCl) (Acros Organics, 99%) and ethylene glycol (EG) (Fisher, 98%). For the reference electrode AgCl (Alfa Aesar, 99.9%) was used. All the chemicals were used as received, without any purification.

The DES used was a mixture of ethylene glycol with choline chloride in a molar ratio of 2:1 (EG:ChCl). For the preparation of the DES, the components were mixed via the heating method in a sealed container, under continuous stirring conditions at 50 ºC, until a transparent

homogeneous liquid was formed. The solvents were then stored at room temperature, in order to slow down any degradation or esterification reaction between the components, since temperature has a great effect on the degradation kinetics of carboxylic acid based-DESs.[41]

Paint casting experiments

All of the cyclic voltammetry, chronopotentiometric and chronocoulometric experiments were carried out using an IVIUMnSTAT multichannel potentiostat/galvanostat together with the corresponding Ivium software. The actual method of paint casting has been reported previously.[40] This method was used for the experiments of cyclic voltammetry, chronopotentiometry and chronocoulometry of solid metal oxide powders in EG:ChCl. The setup of electrodes consisted of a Pt flag *ca.* 0.32 cm^2 serving as the working electrode (WE), Pt flat *ca.* 1 cm^2 acting as counter electrode (CE) and as reference electrode (RE) an Ag wire 1 mm immersed in a saturated solution of AgCl in EG:ChCl. The WE and CE were rinsed with deionized H_2O and dried with acetone prior to use. The metal oxide powder was first ground in a mortar and then mixed with 2 drops of the DES to form a paste, which was then painted onto the WE which was bent at 90º. For the cyclic voltammetry analysis, a minimum amount of metal oxide powder (ca. 1-5 mg) was used to minimise any adverse effects due to the resistivity of the metal oxides. All CVs using metal oxides were started from open circuit potential and swept initially in the anodic direction. Also, before each CV, a linear sweep voltammogram was performed in order to remove any possible contaminants on the surface of the WE. The cyclic voltammogram of pure EG:ChCl was also recorded and shown in Supplementary Information (**Figure S1**). Where redox potentials are discussed, these are taken of an average of oxidation and reduction onset potentials.[42]

For the chronopotentiometry experiments a fixed amount of the paste of the MO (≈ 10 mg) was painted on the WE and the changes in voltage were measured while zero current was passing through the cell for 60 mins. For the chronocoulometry experiments pastes of MOs (≈ 10 mg) were painted on the WE and a fixed potential of 1.2 V vs Ag/AgCl was applied to the cell for 30 mins, at 50 °C.

Electrochemical dissolution of metal oxides

The electrochemical dissolution of MOs was conducted in a cell presented in **Figure S2**. The idea behind this experiment is similar to that of paint casting but on a larger scale and with a configuration of two electrodes instead of three. Both the anode and the cathode were iridium

oxide-coated titanium mesh electrodes. The MO powder was "painted" on the surface of the anode, which was immersed in the DES. The experiments were held at 50 °C and with a liquid to solid (L:S) ratio of 30 at a constant voltage of 2.7 V provided by a bench power supply.

Instrumentation

The metal content of the MO leach solutions was investigated via inductively coupled plasma mass spectrometry (ICP-MS) using a Thermo Scientific iCAP Qc ICP-MS. Each sample was diluted 1000 times in 2 vol% HNO_3. Before the analysis of the samples, calibration lines of each element between 10 and 1000 ppb were determined using a dilutions of a multi-element reference solution 2A (SPEX CertiPrep, 99%). The internal standards (spikes) used in each sample were Rh and La (0.1 ppm).

The speciation analysis of the metals in the pregnant leach solutions was performed using UV-Visible spectroscopy (UV-Vis) on a Mettler Toledo UV5 Bio spectrometer, with a quartz cell of path length 10 mm. In cases where the sample was very concentrated, and where dilution of the sample resulted in a change of colour and hence of metal species, quartz slides with a path length of 0.1 mm were used.

Results and Discussion

Electrochemistry

The first aim is to determine whether the paint casting electro-oxidation method, which has been shown to solubilise a range of sulfides, arsenides and selenides, can also be used to solubilise oxides. To understand the electrochemical behaviour of the cation and anion of the metal oxides, cyclic voltammetry (CV) was carried out using the paint casting method,[43] and the resulting voltammograms displayed in **Figure 1**. The aims were to determine a) whether the oxides are electrochemically active in EG:ChCl, b) the species being oxidised to liberate the metal cations and c) the products of the oxidation process. The CVs for the copper and lead oxides show the same voltammetric behaviour seen for solutions of their respective chloride salts.[5, 44, 45] For copper, the $Cu^{II/I}$ and $Cu^{I/0}$ couples are present at average onset potentials of ca. 0.44 V and ca. -0.37 V vs the 0.1 M Ag/AgCl in DES reference. For lead, the $Pb^{II/0}$ couple is present at ca. -0.54 V, with an additional oxidation peak with an onset potential of ca. -0.33 V relating to the formation of a Pb-Pt alloy.[45, 46] This is most likely due to the fact that these salts are relatively soluble in DESs and the voltammetry will include responses from both the solid oxide and solution-based chloride species.

Different behaviour is observed for Fe_2O_3 and Fe_3O_4, salts which have poorer chemical solubility in EG:ChCl.[29] Here the reversible $Fe^{III/II}$ couple can be seen at ca. +0.37 V vs the 0.1 M Ag/AgCl in DES reference for both systems, but with a reduced current for Fe_2O_3 due to all Fe ions being in the Fe^{III} state initially. There is also an additional quasi-reversible redox event at ca. -0.19 V which is unrelated to the $Fe^{II/0}$ redox couple expected at ca. -0.72 V and is also not observed in solutions of $FeCl_3$ or for paint casted FeS_2.[31] To determine if this unknown redox couple is associated with the metal oxide or the solvent, either due to DES components or dissolved water and oxygen, the CVs were compared to the blank DES (**Figure S3**). In the potential region of the CV of the blank DES where the unknown species is present, there was no significant anodic current recorded. Therefore, it can be reasonably assumed that any oxidative behaviour in this region is due to the metal oxides themselves, or their redox products, instead of the DES components or other species present in the blank.

For the Mn, Co, Ni, and Zn oxides the redox processes relating to $M^{II/0}$ are less clear due to the poorly soluble nature of these salts compared to Cu and Pb, and also their more cathodic redox potentials resulting in the $M^{II/0}$ couple being at similar potentials to the H_2-generating potential window of the solvent. In addition, MnO, CoO, NiO, and ZnO have band gaps of greater than 3.2 eV (see **Table S1**) and can be considered insulators, hence the lower current values recorded. While none of these CVs are particularly well resolved it can be seen that all have a reduction peak at ca. -0.15 to -0.19 V vs the 0.1 M Ag/AgCl in DES reference and an oxidation peak at ca. -0.12 to -0.096 V, similarly to the iron oxides. It must be noted that the CVs of ZnO and $ZnCl_2$ appear different due to the potential ranges used. As the aim was to investigate the oxidation of ZnO, rather than reduction of Zn^{II} to Zn metal, a narrower potential range was selected. In general the smaller the band gap the better the CV is resolved showing the importance of substrate conductivity in the paint casting method.

Similar behaviour has been reported for paint casted lanthanide oxides in EG:ChCl, where CVs of paint casted Er_2O_3, CeO_2, Gd_2O_3, Sm_2O_3, Yb_2O_3 and Pr_2O_3 showed an unidentified reduction peak at ca. -0.2 V and a corresponding oxidation peak at ca. -0.1 V vs Ag/AgCl.[47] Higher paste loadings were determined to increase the current at these potentials as has previously been observed with metal sulfides, indicating that the redox events must be linked to the metal oxide. As the only commonality between all of these systems is the presence of oxide, this redox peak

could be assigned to the formation of electroactive species on the surface of MO, such as superoxide (O_2^-), which could be generated through the oxidation of oxide:

$$2O^{2-} \rightleftharpoons O_2^- + 3e^- \qquad \textbf{Eq. 1}$$

Bulk electrolytic oxidation of metal oxides

Bulk electrolysis enables faster dissolution of metal sulfides and it was shown that the solubilised metal ions could be electrochemically deposited on the counter electrode in a pure state.[31, 48] The same procedure was carried out with MOs which were paint casted onto the iridium oxide-coated titanium mesh anode and dissolved by applying a constant voltage of 2.7 V between the two electrodes for 48 h at 50 °C. It is important to note here that decomposition of the electrolyte during electrolysis must be considered, as it can have an impact on the overall efficiency of the process. It has previously been shown by Haerens et al.[49] that EG:ChCl decomposes during electrolysis at a constant current of 1 A, over a timescale of up to 6 hours. This decomposition resulted in the formation of yellow-coloured decomposition products. In the present work, the current observed during anodic dissolution was in the range of 2 mA, which is not sufficient to cause any major decomposition of the electrolyte. We can therefore assume that any decomposition of the electrolyte is limited. Hence, any changes in colour could be directly attributed to the presence of metal complexes in solution, as will be discussed further.

In **Figure 2**, the concentrations of the dissolved MOs in EG:ChCl after this period are shown and compared with the chemical dissolution in the same solvent, which has been already reported.[29] It is clear that for most MOs, except from Cu_2O and PbO, the electrochemical solubilities are in most cases significantly higher than the chemical solubility. This shows that the solubility of MOs can be significantly enhanced by electrochemical oxidation of the oxide moiety. This shows that the solubility of MOs can be significantly enhanced by electrochemical oxidation. For Fe_2O_3 and Fe_3O_4 the solubility is ca. 18,500 and 51,800 times, higher respectively using electrooxidation than by straight chemical dissolution.

From **Figure 2** it is observed that the concentrations of dissolved Cu_2O and PbO after electrochemical dissolution were lower than after chemical dissolution and for CuO the concentrations were at the same level. It is proposed that this is because both Cu and Pb are very easily electrodeposited so that the metal ions dissolved from the oxide are rapidly deposited on the cathode and thus the solution concentration is does not reflect the total amount

of metal which has been dissolved. As shown in **Figure 3**, a thick grey deposit (15 mg) was formed during PbO anodic dissolution, and a brown deposit (9 mg) formed during CuO and (25 mg) Cu_2O dissolution. EDX measurements showed a metal-to-oxygen ratio in atomic% of 1:1 for the grey deposit, and 4:1 for the brown deposit. There was trace chlorine but no carbon present, indicating that the deposits were mostly free from DES contamination. The other metals do not electrodeposit once they dissolve as it has previously been shown that these metals require a critical concentration typically 50mM before they can be deposited.[50] This provides an appropriate method by which more electropositive metal oxides could be recovered from electronegative metal oxides.

What is worth mentioning is the lack of selectivity of the electrochemical dissolution process in EG:ChCl, i.e. dissolution of the MOs results in roughly similar metal ion concentrations after 48 hr. This supports the hypothesis that dissolution of MOs is driven by the reaction of oxide and not of the metal, and that slight differences between them result from kinetic factors such as MO conductivity and particle size, along with diffusion of solvated products away from the electrode surface. In the case of Cu_2O, the Cu^{I} ion will be oxidised as well, forming Cu^{II}.

Of the metals shown in **Figure 2**, cobalt, and nickel are the more valuable metals and their dissolution is interesting from the perspective of processing lithium ion battery cathode materials. **Figure 4** shows the kinetics of metal ion dissolution. Since the liquids are viscous and the system was unstirred it is not surprising that the dissolution rate increases linearly with the square root of time as would be expected for a diffusion limited process (**Figure 4b)**.[51]

$$\boldsymbol{C = C_o + 2k_p t^{1/2}} \qquad \textbf{Eq. 2}$$

Where C is the concentration of dissolved metal ions, C_0 is the initial concentration of dissolved metal ions, t is the time of reaction, and k_p is the reaction rate constant ($mol \cdot L^{-1} \cdot s^{-1/2}$).

Metal speciation after bulk electrochemical dissolution

In order to determine the speciation of the metal complexes in solution after bulk electrochemical dissolution, UV-Vis spectra were measured and compared to the spectra of known species obtained from chemical dissolution of metal oxides and chlorides.[29, 52] From **Figure 5** it can be clearly seen that the same $[MCl_4]^{2-}$ speciation was retained for the cobalt and lead systems. It is anticipated that zinc will also form the tetrachloride species previously detected,[52, 53] however due to the lack of chromophores in this complex it was not possible to

obtain meaningful UV-Vis data for confirmation of this hypothesis. For the copper system, oxidation of Cu^{I} to Cu^{II} took place, also resulting in formation of the tetrachloride species. The same species have also been observed in solutions obtained from anodic dissolution of copper sulfide compounds,[37] suggesting that metal recovery from oxidised chalcogenide minerals should proceed via the same mechanisms. The higher nickel concentrations generated by electrochemical dissolution of NiO resulted in spectra that can be assigned to the same green $[Ni(EG)_3]^{2+}$ species seen for solutions of nickel chloride in the same DES.[52] Differences between chemical and electrochemical oxidation were seen for the oxides of Mn, where no well-resolved absorbance maxima were observed after chemical dissolution (**Figure S4**). It is however highly likely that any dissolved Mn^{IV} (an oxidising species) will be reduced by reaction with the DES to form the colourless $[MnCl_4]^{2-}$ species that is present after dissolution of chloride salts.

In the case of Fe_3O_4, it is apparent that after anodic dissolution the dark brown solution displays a single maximum at 303 nm, rather than the three peaks typical for spectra of $[FeCl_4]^{-}$. Similar spectra have been reported from the anodic dissolution of pyrrhotite in EG:ChCl, where it was determined that Fe-HBD complexes formed.[38] Additionally, the same peak was observed in an aqueous solution containing glycine after oxidative dissolution of pyrrhotite.[54] For Fe_2O_3 no distinctive peaks are observed at the UV-Vis spectra, despite having similar concentrations of Fe to the solution of Fe_3O_4. It is therefore likely that a different species with a smaller molar extinction coefficient is present, or that the Fe forms a colloidal species that can slowly precipitate over time.

Superoxide is a difficult species to generate or detect reproducibly[55] but one method that has been repeatedly used is UV-Vis spectroscopy, where it is known to absorb in the range of 255-275 nm.[56] To investigate this without interference from the cation the electrolysis of KO_2 was carried out in EG:ChCl and UV-Vis spectra were recorded (**Figure S5**). The solutions were prepared and measured on the same day to minimise any effects of superoxide instability in the DES. A single peak is observed at around 279 nm, which is close to the already published values for superoxide in other solvents. The use of KO_2 for the localization of superoxide in solution is common in aqueous solutions, where the peak attributed to O_2^{-} is at 245 nm in water and 255 in acetonitrile.[55] This apparent stability of superoxide in EG:ChCl over the course of a few hours gives weight to the possibility that superoxide can be generated in DES media from

anodic dissolution of metal oxides. In future it would be important to examine the maximum lifetime of this species in DESs.

Discussion of the superoxide hypothesis

From the voltammetry, it is proposed that the oxidative dissolution of MOs in EG:ChCl takes place via oxidation of the oxide moiety, resulting in the formation of a reactive superoxide species on the surface of the bulk MO. If there is a higher oxidation state available for the metal ion within the potential window of the experiment, the metal ion will be oxidised too, as in the case of Cu_2O. **Equation 3** shows the proposed mechanism of dissolution for the example of ZnO:

$$\mathbf{2ZnO + 8Cl^- \longrightarrow 2[ZnCl_4]^{2-} + [O_2^-] + 3e^-} \qquad \textbf{Eq. 3}$$

Oxide (O^{2-}) can be oxidised to the radical superoxide species (O_2^-) by the process shown in equation 1. A second oxidation step could be the oxidation or decomposition of superoxide to oxygen gas (O_2). The proposal that the driving force of the electrochemical dissolution is the oxidation of the non-metal part of the MO follows because many of the MOs are either in their highest oxidation state or do not have another oxidation state e.g. ZnO. The metal ion cannot lose any further electrons, hence cannot be oxidised. Similar behaviour has been seen for other chalcogenide systems, where the sulfide moiety is oxidised to elemental sulfur and sulfate during anodic dissolution of copper and iron sulphides.[38, 48]

Superoxides have been mostly studied as the product of the oxygen reduction reaction, where oxygen can take one electron and form superoxide.[55] The formation of the radical superoxide by the oxidation of oxide is not that widely studied or understood, as superoxide is unstable in most solutions, especially in water, where the solvation is very high and disproportionation occurs at a rapid rate (10^7 - 10^{10} $mol^{-1}\cdot L\cdot s^{-1}$).[55, 57] It is reported and expected that superoxide radicals with unpaired electrons are highly reactive in many solvents.[55] However, higher stability has been seen in some aprotic solvents such as acetone and pyridine, and a lower reactivity in isopropanol.[58] To some extent the stability of the superoxide is not important if the metal-oxygen bond is changed, which enables the metal to be released into solution, as will happen during bulk electrolysis.

It is therefore proposed here that, during the electrochemical oxidation of MOs in EG:ChCl, the oxidation of oxide to superoxide occurs, overcoming the lattice energy of the MO to enable

the formation of chloro complexes. From comparing total charge passed to bandgap, it can be seen that there is a negative correlation, indicating that smaller band gaps result in greater dissolution due to less charge lost due to resistivity (**Figure 6**). The effect of the band gap on the reactivity of semiconductors and minerals has been previously proposed. Since the band gap is the energy difference between the filled valence band and the empty conduction band, its size will have an effect on the reactivity of minerals and the ease of the electron transfer from the valence to the conduction band. Crundwell suggested that the band gap of sulfide minerals will have an effect on the way through which the minerals will dissolve and the rate of the dissolution.[59] For semiconductors with a band gap >1 eV the anodic dissolution proceeds through a hole injection in the valence band, whereas for semiconductors with band gap <1 eV the dissolution occurs with the contribution of both electrons in the conduction band and holes in the valence band. The correlation observed in **Figure 6** should probably be viewed as a general trend. It has been previously observed for the dissolution of sulfides in DESs[38, 39] but the correlation assumes that the process is 100% current efficient, and the charge is the same for the dissolution of one mole of each metal. If the rate was a function of the band gap, it might also be expected to be an exponential (Arrhenius) correlation rather than a linear function so it is probably safer to describe a general trend for faster dissolution rate of materials with lower band gaps.

Conclusions

This study shows that a range of metal oxides are electrochemically active in DES media. It has been shown that all the metal oxides studied could be solubilised through electrooxidation and some of the metals could be recovered in a pure form on the counter electrode, indicating a potential methodology to recover metals from minerals or end of life materials such as battery electrodes. The dissolution mechanism appears to be driven by oxidation of the oxide to a species we suspect to be the superoxide, which is sufficiently long-lived (at least 24 hr) to be visible in the UV-Vis spectrum but will ultimately decompose to an as yet unidentified product. The metal ions released form similar complexes to those seen from the dissolution of metal halides and metal sulfides suggesting that the oxide does not remain attached to the metal upon dissolution. Electrochemical dissolution of some oxides resulted in >10,000 times higher solubility than chemical dissolution over a similar time period. The dissolution under the experimental conditions used was found to be mass transport controlled.

Conflicts of interest

There are no conflicts of interest to declare

Acknowledgements

The authors would like to thank the European Commission's H2020 – Marie Sklodowska Curie Actions (MSCA) − Innovative Training Networks for the funding received within the SOCRATES project under the grant agreement no. 721385 (Project website: http://etn-socrates.eu). The authors would also like to thank the Faraday Institution (grant codes FIRG005 and FIRG006) for funding (Project website https://relib.org.uk).

ORCID numbers:

Ioanna Maria Pateli: 0000-0001-5582-7767

Andrew Abbott: 0000-0001-9556-8341

Gawen Jenkin: 0000-0001-9202-7128

Jennifer Hartley: 0000-0003-2174-4458

Figures and Tables

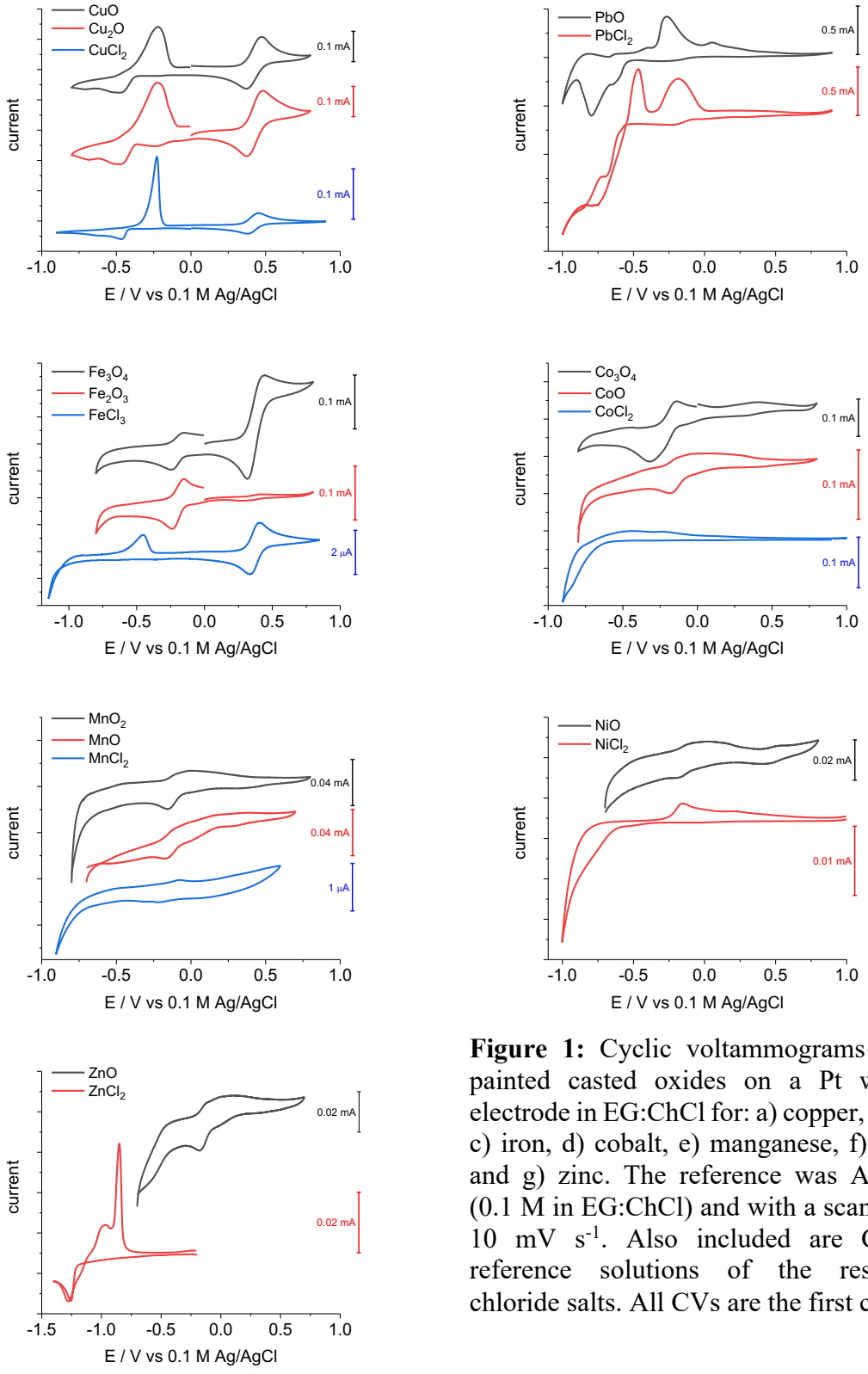

Figure 1: Cyclic voltammograms of the painted casted oxides on a Pt working electrode in EG:ChCl for: a) copper, b) lead, c) iron, d) cobalt, e) manganese, f) nickel, and g) zinc. The reference was Ag/AgCl (0.1 M in EG:ChCl) and with a scan rate of 10 mV s^{-1}. Also included are CVs of reference solutions of the respective chloride salts. All CVs are the first cycle.

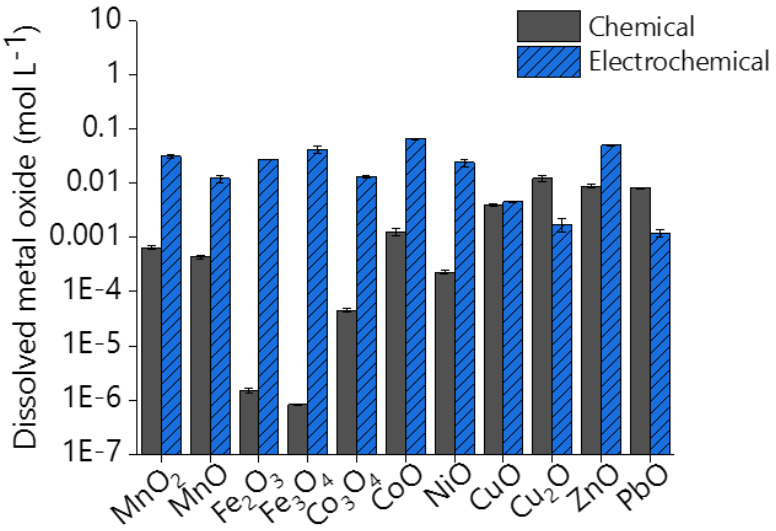

Figure 2: Comparison of chemical and electrochemical dissolution of metal oxides in EG:ChCl. Conditions for electrochemical dissolution: T = 50 °C, t = 48 hours, L:S = 30, constant applied of 2.7 V. Values of chemical dissolution are taken from ref [29]

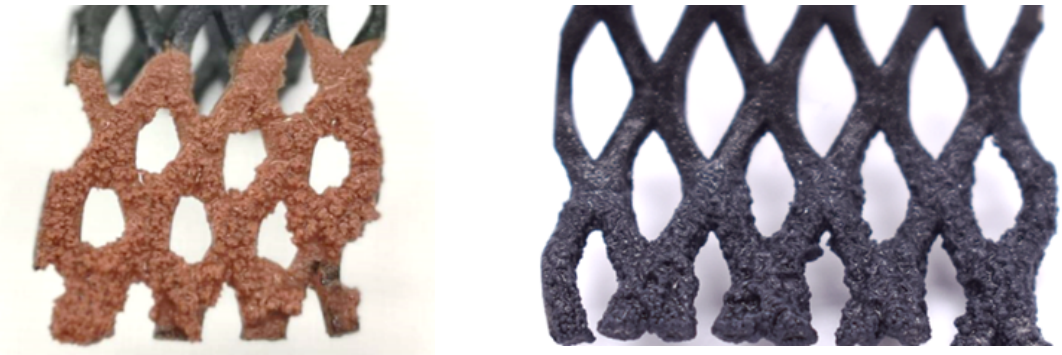

Figure 3: Material deposited on the cathode after electrochemical dissolution of Cu_2O (left) and PbO (right) in EG:ChCl.

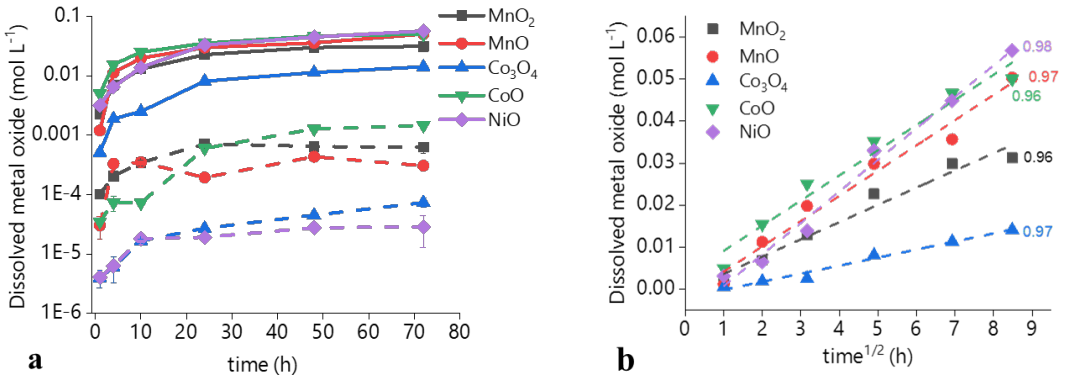

Figure 4: a) Kinetic studies of selected MOs after electrochemical dissolution (solid lines) and chemical dissolution (dashed lines) in EG:ChCl. b) Diffusion model plot of concentration depending on time for the electrochemical dissolution, with correlation coefficients. Conditions for electrochemical dissolution: T = 50 °C, L:S=30, and constant V = 2.7 V.

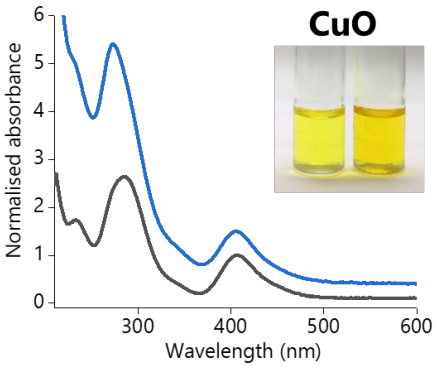
CuO
Normalised absorbance
Wavelength (nm)

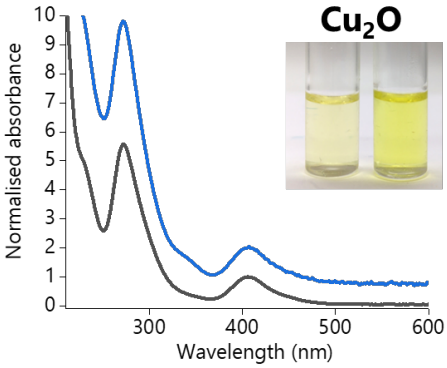
Cu2O
Normalised absorbance
Wavelength (nm)

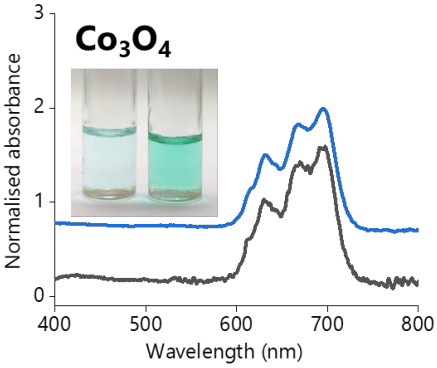
Co3O4
Normalised absorbance
Wavelength (nm)

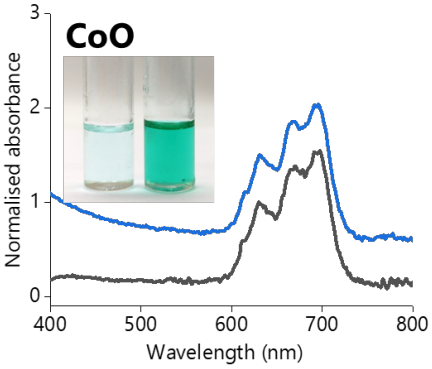
CoO
Normalised absorbance
Wavelength (nm)

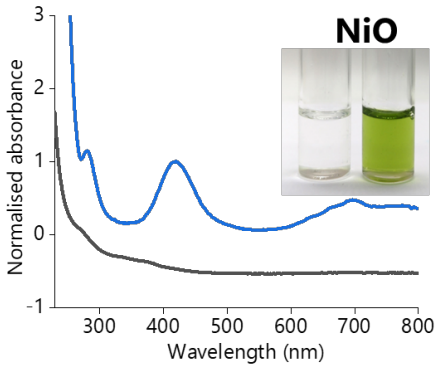
NiO
Normalised absorbance
Wavelength (nm)

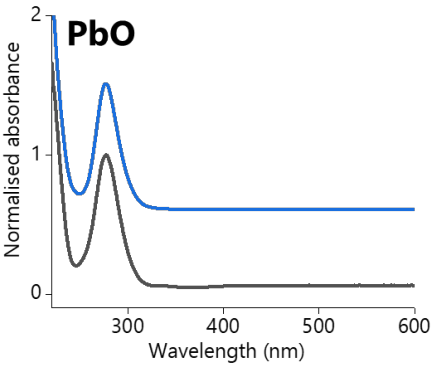
PbO
Normalised absorbance
Wavelength (nm)

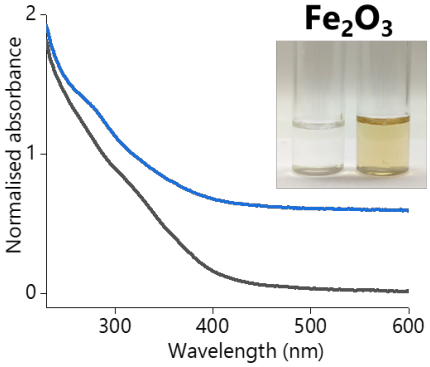
Fe2O3
Normalised absorbance
Wavelength (nm)

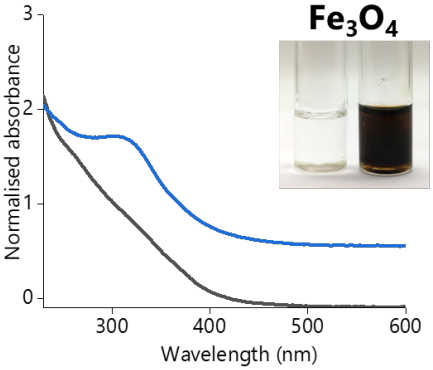
Fe3O4
Normalised absorbance
Wavelength (nm)

Figure 5: UV-Vis spectra of metal oxides in EG:ChCl after chemical (black) and electrochemical (blue) dissolution. Inset: the obtained solutions obtained after chemical (left) and electrochemical dissolution (right).

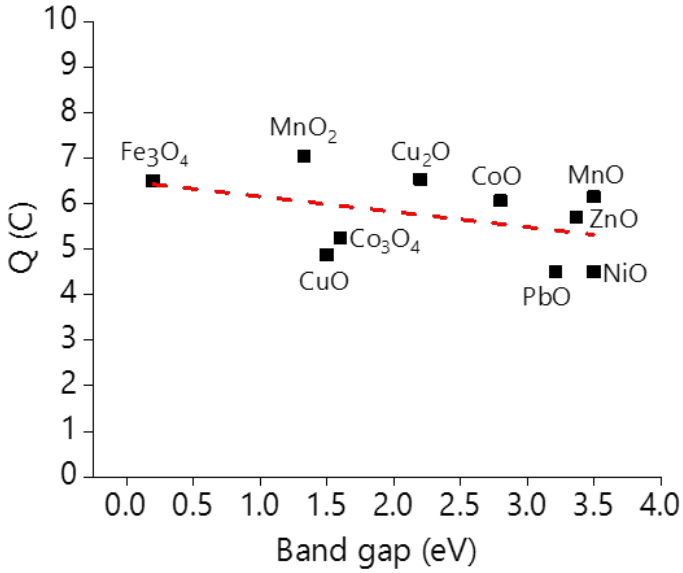

Figure 6: Effect of the band gap of metal oxides on the total charge passed during chronocoulometry.

References

1. D. Cheret and S. Stanten, Battery recycling. U.S. Patent No. 7,169,206., 2007.
2. T. Norgate, S. Jahanshahi and W. Rankin, *Journal of Cleaner Production*, 2007, **15**, 838-848.
3. A. P. Abbott, G. Frisch, J. Hartley and K. S. Ryder, *Green Chemistry*, 2011, **13**, 471-481.
4. K. Binnemans and P. T. Jones, *Journal of Sustainable Metallurgy*, 2017, **3**, 570-600.
5. A. P. Abbott, G. Frisch, S. J. Gurman, A. R. Hillman, J. Hartley, F. Holyoak and K. S. Ryder, *Chemical Communications*, 2011, **47**, 10031-10033.
6. E. L. Smith, A. P. Abbott and K. S. Ryder, *Chemical Reviews*, 2014, **114**, 11060-11082.
7. F. Endres, A. Abbott and D. R. MacFarlane, *Electrodeposition from ionic liquids*, John Wiley & Sons, 2017.
8. S. Dai, Y. S. Shin, L. M. Toth and C. E. Barnes, *Inorganic Chemistry*, 1997, **36**, 4900-4902.
9. R. C. Bell, A. Castleman and D. Thorn, *Inorganic Chemistry*, 1999, **38**, 5709-5715.
10. P. Nockemann, B. Thijs, S. Pittois, J. Thoen, C. Glorieux, K. Van Hecke, L. Van Meervelt, B. Kirchner and K. Binnemans, *Journal of Physical Chemistry B*, 2006, **110**, 20978-20992.
11. P. Nockemann, B. Thijs, T. N. Parac-Vogt, K. Van Hecke, L. Van Meervelt, B. Tinant, I. Hartenbach, T. Schleid, V. T. Ngan, M. T. Nguyen and K. Binnemans, *Inorganic Chemistry*, 2008, **47**, 9987-9999.
12. S. Wellens, T. Vander Hoogerstraete, C. Möller, B. Thijs, J. Luyten and K. Binnemans, *Hydrometallurgy*, 2014, **144-145**, 27-33.
13. D. Dupont, S. Raiguel and K. Binnemans, *Chemical Communications*, 2015, **51**, 9006-9009.
14. P. Davris, E. Balomenos, D. Panias and I. Paspaliaris, *Hydrometallurgy*, 2016, **164**, 125-135.
15. F.-L. Fan, Z. Qin, S.-W. Cao, C.-M. Tan, Q.-G. Huang, D.-S. Chen, J.-R. Wang, X.-J. Yin, C. Xu and X.-G. Feng, *Inorganic Chemistry*, 2018, **58**, 603-609.
16. A. P. Abbott, G. Capper, D. L. Davies, R. K. Rasheed and P. Shikotra, *Inorganic Chemistry*, 2005, **44**, 6497−6499.
17. A. P. Abbott, G. Capper, D. L. Davies, K. J. McKenzie and S. U. Obi, *Journal of Chemical and Engineering Data*, 2006, **51**, 1280-1282.

18. A. Abbott, G. Capper, D. Davies and P. Shikotra, *Mineral Processing and Extractive Metallurgy*, 2006, **115**, 15-18.

19. D. Dupont and K. Binnemans, *Green Chemistry*, 2015, **17**, 856-868.

20. S. Riaño, M. Petranikova, B. Onghena, T. Vander Hoogerstraete, D. Banerjee, M. R. S. Foreman, C. Ekberg and K. Binnemans, *RSC Advances*, 2017, **7**, 32100-32113.

21. N. Rodriguez Rodriguez, L. Machiels and K. Binnemans, *ACS Sustainable Chemistry & Engineering*, 2019, **7**, 3940-3948.

22. A. Söldner, J. Zach and B. König, *Green Chemistry*, 2019, **21**, 321-328.

23. P. Zürner and G. Frisch, *ACS Sustainable Chemistry and Engineering*, 2019, **7**, 5300-5308.

24. A. D. Ballantyne, J. P. Hallett, D. J. Riley, N. Shah and D. J. Payne, *Royal Society open science*, 2018, **5**, 171368.

25. M. K. Tran, M.-T. F. Rodrigues, K. Kato, G. Babu and P. M. Ajayan, *Nature Energy*, 2019, **4**, 339.

26. G. Damilano, A. Laitinen, P. Willberg-Keyriläinen, T. Lavonen, R. Häkkinen, W. Dehaen, K. Binnemans and L. Kuutti, *RSC Advances*, 2020, **10**, 23484-23490.

27. N. Peeters, K. Binnemans and S. Riaño, *Green Chemistry*, 2020.

28. I. M. Pateli, A. P. Abbott, K. Binnemans and N. Rodriguez Rodriguez, *RSC Advances*, 2020, **10**, 28879-28890.

29. I. M. Pateli, D. Thompson, S. S. M. Alabdullah, A. P. Abbott, G. R. T. Jenkin and J. M. Hartley, *Green Chemistry*, 2020, **22**, 5476-5486.

30. M. Pourbaix, *Atlas of Electrochemical Equilibria in Aqueous Solutions*, NACE International & Celebcor, Houston, Texas, USA & Brussels, 1974.

31. A. P. Abbott, A. Z. M. Al-Bassam, A. Goddard, R. C. Harris, G. R. T. Jenkin, F. J. Nisbet and M. Wieland, *Green Chemistry*, 2017, **19**, 2225-2233.

32. G. Z. Chen, D. J. Fray and T. W. Farthing, *Nature*, 2000, **407**, 361-364.

33. J.-M. Hur, C.-S. Seo, S.-S. Hong, D.-S. Kang and S.-W. Park, *Reaction Kinetics and Catalysis Letters*, 2003, **80**, 217-222.

34. K. Mohandas and D. Fray, *Trans. Indian Inst. Met*, 2004, **57**, 579-592.

35. Q. Zhang, R. Wang, K. Chen and Y. Hua, *Electrochimica Acta*, 2014, **121**, 78-82.

36. J. Ru, Y. Hua, D. Wang, C. Xu, J. Li, Y. Li, Z. Zhou and K. Gong, *Electrochimica Acta*, 2015, **186**, 455-464.

37. S. Anggara, F. Bevan, R. C. Harris, J. M. Hartley, G. Frisch, G. R. T. Jenkin and A. P. Abbott, *Green Chemistry*, 2019, **21**, 6502-6512.

38. J. M. Hartley, A. Z. M. Al-Bassam, R. C. Harris, G. Frisch, G. R. T. Jenkin and A. P. Abbott, *Hydrometallurgy*, Accepted manuscript number HYDROM_2020_574R1, 2020.

39. F. Bevan, *Electrochemical Processing of Metal Chalcogenides in Deep Eutectic Solvents*, PhD thesis, University of Leicester, 2019.

40. A. P. Abbott, F. Bevan, M. Baeuerle, R. C. Harris and G. R. Jenkin, *Electrochemistry Communications*, 2017, **76**, 20-23.

41. N. Rodriguez Rodriguez, A. van den Bruinhorst, L. J. Kollau, M. C. Kroon and K. Binnemans, *ACS Sustainable Chemistry & Engineering*, 2019, **7**, 11521-11528.

42. N. Frenzel, J. Hartley and G. Frisch, *Phys Chem Chem Phys*, 2017, **19**, 28841-28852.

43. A. P. Abbott, F. Bevan, M. Baeuerle, R. C. Harris and G. R. T. Jenkin, *Electrochemistry Communications*, 2017, **76**, 20-23.

44. A. P. Abbott, K. El Ttaib, G. Frisch, K. J. McKenzie and K. S. Ryder, *Physical Chemistry Chemical Physics*, 2009, **11**, 4269-4277.

45. Y.-S. Liao, P.-Y. Chen and I. W. Sun, *Electrochimica Acta*, 2016, **214**, 265-275.

46. Y. Katayama, R. Fukui and T. Miura, *Journal of The Electrochemical Society*, 2013, **160**, D251-D255.

47. S. Stodd, *Lanthanide processing in Deep Eutectic Solvents*, PhD thesis, University of Leicester, 2018.

48. S. Anggara, F. Bevan, R. C. Harris, J. Hartley, G. Frisch, G. Jenkin and A. P. Abbott, *Green Chemistry*, 2019, **21**, 6502-6512.

49. K. Haerens, E. Matthijs, K. Binnemans and B. Van der Bruggen, *Green Chemistry*, 2009, **11**, 1357–1365.

50. H. F. Alesary, S. Cihangir, A. D. Ballantyne, R. C. Harris, D. P. Weston, A. P. Abbott and K. S. Ryder, *Electrochimica Acta*, 2019, **304**, 118-130.

51. W. Stumm and R. Wollast, *Reviews of Geophysics*, 1990, **28**, 53-69.

52. J. M. Hartley, C. M. Ip, G. C. Forrest, K. Singh, S. J. Gurman, K. S. Ryder, A. P. Abbott and G. Frisch, *Inorganic Chemistry*, 2014, **53**, 6280-6288.

53. A. P. Abbott, J. C. Barron, G. Frisch, S. Gurman, K. S. Ryder and A. Fernando Silva, *Phys Chem Chem Phys*, 2011, **13**, 10224-10231.

54. M. I. Duinea, A. M. Sandu, M. A. Petcu, I. Dăbuleanu, G. Cârâc and P. Chiriță, *Journal of Electroanalytical Chemistry*, 2017, **804**, 165-170.

55. M. Hayyan, M. A. Hashim and I. M. AlNashef, *Chemical Reviews*, 2016, **116**, 3029-3085.

56. M. Hayyan, F. S. Mjalli, I. M. AlNashef and M. A. Hashim, *Int. J. Electrochem. Sci.*, 2012, **7**, 9658-9667.

57. M. J. Moorcroft, C. E. Hahn and R. G. Compton, *Journal of Electroanalytical Chemistry*, 2003, **541**, 117-131.

58. M. Mohammad, A. Khan, M. Subhani, N. Bibi, S. Ahmad and S. Saleemi, *Research on Chemical Intermediates*, 2001, **27**, 259-267.

59. F. K. Crundwell, *Hydrometallurgy*, 1988, **21**, 155-190.

Electrochemical oxidation as alternative for dissolution of metal oxides in deep eutectic solvents

Ioanna M. Pateli,[a,b] Andrew P. Abbott,[a] Gawen R. T. Jenkin,[c] Jennifer M. Hartley [a]*

[a] School of Chemistry, University of Leicester, Leicester, LE1 7RH, UK

[b] Stephenson Institute for Renewable Energy, University of Liverpool, Liverpool, L69 7ZF, UK

[c] School of Geography, Geology and the Environment, University of Leicester, Leicester, LE1 7RH, UK

Supplementary information:

Chronocoulometry and open circuit potential measurements

Chronocoulometry measures the charge passed through an electrode as a function of time at a fixed potential and gives a measure of process kinetics. This process has been tested for iron sulfide and arsenide minerals in DES media, where it was shown that charge passed was correlated to the band gap of the minerals, with a smaller band gap resulting in faster dissolution rates, but only within the anion groupings.[1, 2] Applying this to a selection of d-block metal oxides and PbO results in the same general trend applying, i.e. the more conducting oxides are more easily oxidised than the more insulating oxides. From this limited selection of metal oxides there does not appear to be any trend for oxidation state or periodic group.

Open circuit potential (OCP) measurements were carried out on MO paste in EG:ChCl to examine the stability of the MOs and their tendency to chemically dissolve (**Table 1** & Error! Reference source not found.). The MOs investigated can be divided into two groups: those that remain stable even after one hour (Fe_3O_4, Co_3O_4 and NiO), and those that show a decrease in potential with time (CuO, Cu_2O, ZnO and PbO). When the OCP value of the electrode is stable with respect to time, the equilibrium established between the MO and the electrolyte is relatively stable, i.e. resistant to corrosion reactions from the surrounding electrolyte. On the other hand, when the OCP changes over time it shows that the MO is

prone to chemical dissolution in the electrolyte, as the changing metal ion concentration in solution affects the potential. However, OCP values do not correlate to chronocoulometry or band gap values.

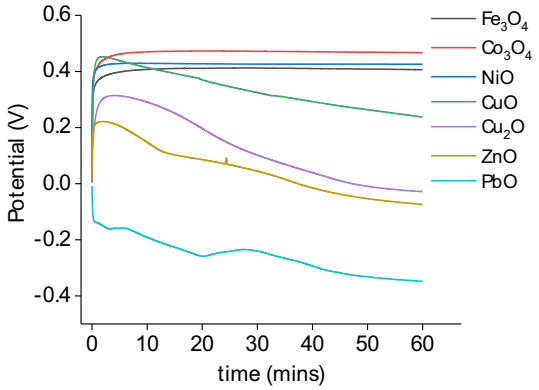

Figure S1: Open circuit potential of metal oxides paint casted in EG:ChCl, with a 0.32 cm^2 Pt flag WE, a Pt flag CE and an Ag/AgCl (0.1 M in EG:ChCl) reference electrode.

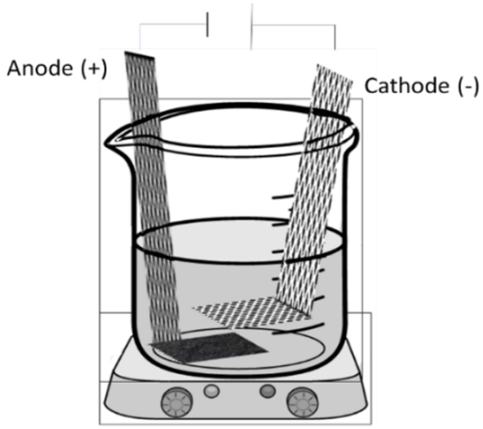

Figure S2: Schematic representation of the cell used for bulk electrochemical dissolution of metal oxides in DES media. A slurry of the metal oxide is pasted onto the anode.

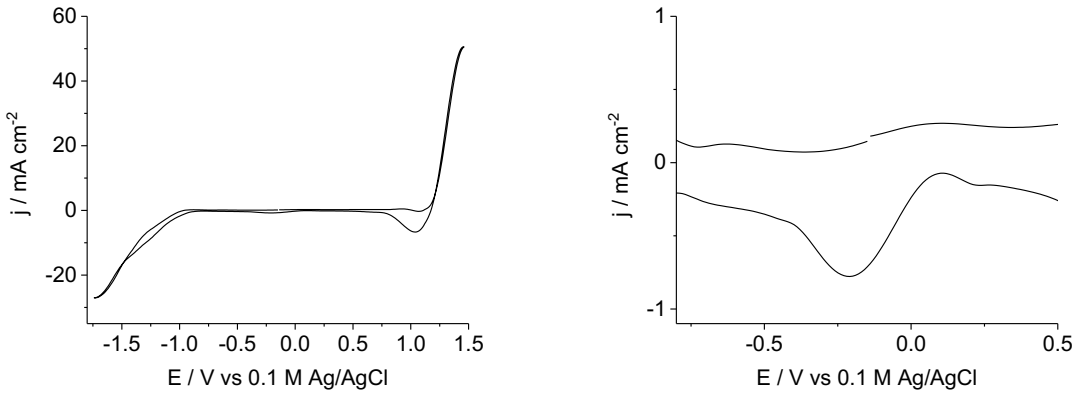

Figure S3: Cyclic voltammogram of pure EG:ChCl with a Pt disc WE, a Pt flag CE and an Ag/AgCl (0.1 M in EG:ChCl) RE. Scan rate: 5 mV s^{-1} (right: zoomed-in "superoxide" region). The cathodic decomposition reaction is likely evolution of H_2 gas, whereas the anodic decomposition reaction is likely evolution of O_2 and/or Cl_2 gas. A reductive process can be seen in the suspected "superoxide" region, of perhaps dissolved O_2 to either superoxide O_2^- or oxide O^{2-} species; however, no corresponding oxidation process is present, indicating that no superoxide is generated during the oxidative sweep, i.e. species is too short-lived or diffuses into the bulk during the timescale of the experiment.

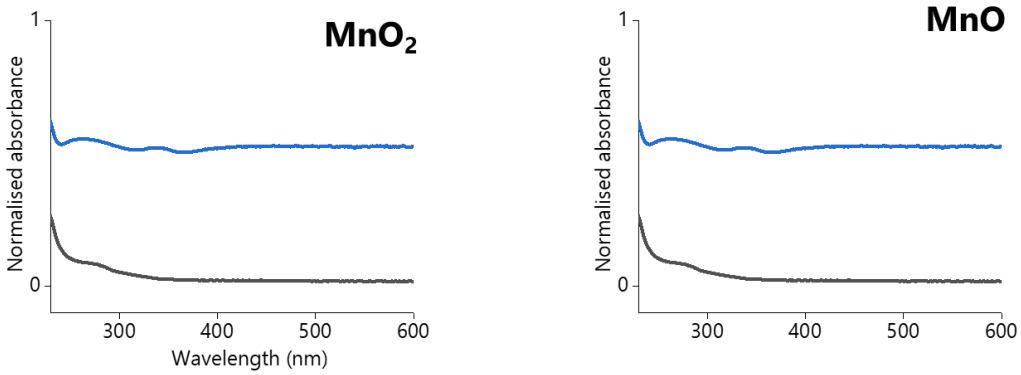

Figure S4: UV-Vis spectra of manganese oxides in EG:ChCl after chemical (black) and electrochemical (blue) dissolution.

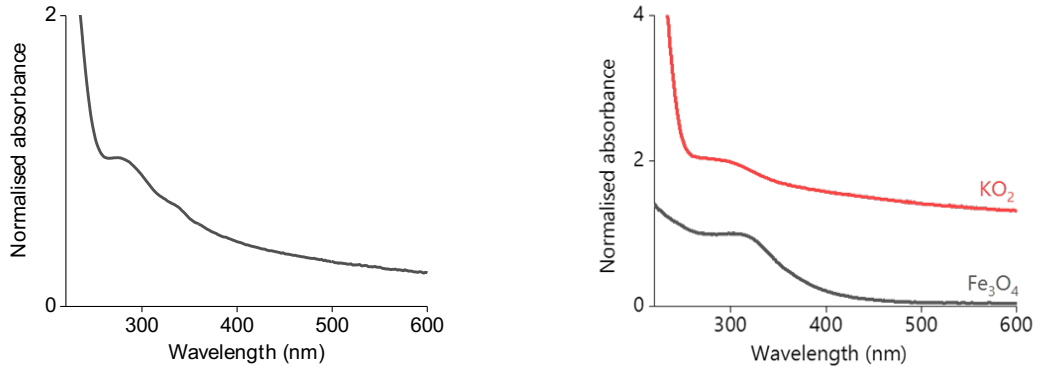

Figure S5: UV-Vis spectra of solution of KO_2 after chemical dissolution in EG:ChCl (left), and compared to the solution obtained from anodic dissolution of Fe_3O_4 (right).

Table 1: Band gap, dissolution rate, and OCP values for selected metal oxides in EG:ChCl.			
Metal Oxide	**Band Gap (eV)**	**Q (C)**	**OCP (V)**
Fe_3O_4	0.2 [3]	6.5	0.406
MnO_2	1.33 [4]	7	-
CuO	1.6 [5]	5.2	0.237
Cu_2O	2.2 [5]	6.5	-0.028
Fe_2O_3	2.2 [6]	2.2	-
Co_3O_4	2.4 [5]	4.8	0.467
PbO	3.21 [7]	4.5	-0.348
CoO	3.3 [5]	6.0	-
ZnO	3.37 [8]	5.7	-0.074
NiO	3.5 [5]	4.5	0.426
MnO	3.5 [5]	6.14	-

References

1. A. P. Abbott, A. Z. M. Al-Bassam, A. Goddard, R. C. Harris, G. R. T. Jenkin, F. J. Nisbet and M. Wieland, *Green Chemistry*, 2017, **19**, 2225-2233.
2. A. Z. M. Al-Bassam, J. M. Hartley, R. C. Harris, G. Frisch, G. R. T. Jenkin and A. P. Abbott, unpublished work.

3. H. Liu and C. Di Valentin, *The Journal of Physical Chemistry C*, 2017, **121**, 25736-25742.
4. S. LeBlanc and H. S. Fogler, *AIChE journal*, 1986, **32**, 1702-1709.
5. S. Lany, *Physical Review B*, 2013, **87**, 085112.
6. B. Gilbert, C. Frandsen, E. R. Maxey and D. M. Sherman, *Physical Review B*, 2009, **79**.
7. H. J. Terpstra, R. A. De Groot and C. Haas, *Physical Review B*, 1995, **52**, 11690-11697.
8. C. Klingshirn, *physica status solidi (b)*, 1975, **71**, 547-556.